

Sodium atoms and clusters on graphite: a density functional study

K. Rytönen¹, J. Akola², and M. Manninen¹

¹*Department of Physics, University of Jyväskylä, FIN-40351 Jyväskylä, Finland and*

²*Institut für Festkörperforschung, Forschungszentrum Jülich, D-52425 Jülich, Germany*

(Dated: July 17, 2018)

Abstract

Sodium atoms and clusters ($N \leq 5$) on graphite (0001) are studied using density functional theory, pseudopotentials and periodic boundary conditions. A single Na atom is observed to bind at a hollow site 2.45 Å above the surface with an adsorption energy of 0.51 eV. The small diffusion barrier of 0.06 eV indicates a flat potential energy surface. Increased Na coverage results in a weak adsorbate-substrate interaction, which is evident in the larger separation from the surface in the cases of Na₃, Na₄, Na₅, and the (2×2) Na overlayer. The binding is weak for Na₂, which has a full valence electron shell. The presence of substrate modifies the structures of Na₃, Na₄, and Na₅ significantly, and both Na₄ and Na₅ are distorted from planarity. The calculated formation energies suggest that clustering of atoms is energetically favorable, and that the open shell clusters (e.g. Na₃ and Na₅) can be more abundant on graphite than in the gas phase. Analysis of the lateral charge density distributions of Na and Na₃ shows a charge transfer of ~ 0.5 electrons in both cases.

I. INTRODUCTION

Graphite is a semimetal that is widely utilized in experimental surface physics. The planar geometry and weak van der Waals -type interlayer interaction make it possible to split flat, chemically inert, and clean graphite (0001) surfaces (highly oriented pyrolytic graphite, HOPG), which are ideal for studying adsorption layers and clusters. The electronic 2D semimetal properties of graphite are well-known both experimentally and theoretically. For instance, density functional theory (DFT) has provided information about the valence charge density, electronic density of states, band structure, elastic constants, and equation of state.^{1,2,3,4}

An interesting research field considers alkali metal atoms and clusters on graphite. Reactivity and metallic properties make alkali metals exciting both for nanotechnological applications and basic science, and the properties of adsorbed alkali metal atoms on HOPG evolve as a function of coverage. Initially, a dispersed and highly polarized phase (“correlated liquid”) is found where alkali atoms maintain a maximum distance between each other. After a critical density of adatoms is reached, a nucleation to more closely packed configurations (islands) occurs.⁵ Alkali metals seem to have a higher charge transfer to HOPG with lower coverage, and an increase in adatom density tends to re-organize the charge into the alkali metal layer forming a two-dimensional metallic state that has a small surface corrugation and is almost decoupled from the substrate.^{5,6,7,8,9} It has been proposed that alkali-metal-plated graphite could have practical applications as a substrate in studying normal and superfluid He films.^{6,10}

Despite the similar electronic structure of alkali metals, deviations in island formation and interaction with HOPG are observed as the atomic number increases. While lithium atoms either intercalate between the graphene layers⁴ or form a planar incommensurate hcp superstructure on HOPG,¹¹ it has been suggested that sodium nucleates only in buckled (110) bcc overlayers.^{12,13} The larger alkali atoms (K,Ru,Cs) are found to intercalate via surface defects^{6,9} or to adsorb in a (2×2) phase occupying hollow sites of the hexagonal substrate.^{6,9,14,15} In addition, cesium can exist in an incommensurate hexagonal or a more sparse $(\sqrt{7} \times \sqrt{7})R19.11^\circ$ phase,^{6,14,15} and a dense $(\sqrt{3} \times \sqrt{3})R30^\circ$ structure has been proposed for potassium.¹⁶ Obviously, the above observations are related to the atomic radius and ionization potential of the alkali atom in question, which affect both the adatom-adatom

and adatom-surface interactions.

The first experimental studies considered metal islands and metal-layers on graphite. A more controlled treatment of adsorbates is challenging, and it is difficult to study separated atoms and size-selected small clusters. Contemporary experimental techniques are able to deal with the practical difficulties such as the substrate temperature, surface defects, kinetic energy of cluster deposition (“soft-landing”), and cluster aggregation.¹⁸ Theoretical studies concern mostly single atoms^{19,20,21,22} or atomic layers on graphite formed by periodic boundary conditions.^{7,8,23} However, research on supported clusters is needed because they form a bridge between isolated atoms and ordered nanolayers, and they may have nanotechnological importance (quantum dots, catalysis). Several attempts to model small clusters and molecules on HOPG have been made,^{8,20,21,24,25,26,27,28,29} but the large number of substrate atoms and the semimetallic nature of graphite (\mathbf{k} -points) make reliable calculations very demanding.

Various theoretical methods are capable of studying metal atoms and clusters on graphite (0001). In addition to deciding which theoretical tools to use, a crucial question is how to model a graphite surface, i.e., how many graphene layers are needed, how large should the substrate be, and does the adsorbate change the surface geometry? One approach is to place the metal cluster under study onto an isolated hydrogen-terminated piece of graphite (“cluster”) that mimics a continuous surface.^{19,20,21,29} The question then is how large should the graphite cluster be in order to get realistic results? On the other hand, there is a problem in optimizing the geometry of the substrate if several graphene layers are involved. This is due to the fact that the layers are interlocked, and the system (Bernal graphite, stacking ABAB) is not fully symmetric at the substrate edges. With periodic boundary conditions one can describe, in principle, a continuous infinite system (“slab”) in the lateral dimensions. In this case, the problem is the distance between adsorbate replicas, which should be large enough to exclude charge density overlap. The large substrate that must be used increases the computational cost greatly.

In the present work, a DFT method with periodic boundary conditions has been used to model Na atoms and clusters ($N \leq 5$) on HOPG. The substrate consisted of three graphene layers with 32 (60) carbon atoms each. It was found that the HOPG potential energy surface (PES) is very flat with the hollow site of the carbon hexagonal structure being preferred. Although alkali metal atoms tend to be more weakly bound to the surface when the coverage

increases, this tendency is not so clear in small Na clusters. The calculated cluster energetics favor clustering processes on HOPG, and the stability of open shell clusters (Na_3 and Na_5) is increased.

II. SIMULATION METHODS

The calculations have been performed using the Car-Parrinello molecular dynamics (CPMD) package,³⁰ which is based on density functional theory. The electron-ion interaction is described by ionic pseudopotentials having the non-local, norm-conserving, and separable form suggested by Troullier and Martins.³¹ Periodic boundary conditions are employed, and the plane wave basis has a kinetic energy cut-off of 70 Ry. The generalized gradient-corrected approximation of Perdew, Burke and Ernzerhof (PBE)³² is adopted for the exchange-correlation energy density. The electronic Hamiltonian is re-diagonalized after each geometry optimization step, and a finite temperature functional ($T = 1000$ K) is used for the Kohn-Sham (KS) orbital occupancies due to the small energy gap between the occupied and unoccupied states (band gap). The ionic positions are optimized using a conjugate gradient method until all the components of nuclear gradient are below 1×10^{-4} a.u.

We model two periodic substrates of Bernal graphite which consist of three graphene layers (stacking ABA) in orthorhombic supershells of $9.84 \times 8.53 \times 16.70$ (96 C atoms) and $12.30 \times 12.79 \times 16.70 \text{ \AA}^3$ (180 C atoms). The smaller substrate with Na_3 is shown in Fig. 1 from two perspectives. Our tests for different numbers of graphene layers have shown that at least three layers are needed in order to reach a convergence in Na adsorption.³⁴ The spacing between the layers is fixed to the experimental value 3.35 \AA , since the PBE functional used has problems in describing weak van der Waals-type interactions.⁴ The choice of z -dimension keeps the slab replica 10 \AA apart, which is sufficient for most applications. However, a weak binding of Na_2 (and large separation from the surface) forced us to use 2 \AA larger spacing in this case. For Na_4 and Na_5 the interaction between cluster replicas becomes significant in the smaller box, and a larger substrate in x - and y -dimensions is needed, where the minimum distance between the clusters is now 7.62 and 6.53 \AA , respectively.

Extensive tests for different numbers of \mathbf{k} -points have shown that the simple Γ -point approximation is not reliable for the systems studied. This is manifested by an artificial planar elongation of the graphite hexagons during geometry optimization, and is probably

related to a strong downward dispersion of the upper σ bands at the Γ -point.^{1,2} The problem does not occur with a $2\times 2\times 1$ Monkhorst-Pack \mathbf{k} -point mesh, and a variation of lateral dimension results in a value 1.421 Å for the C-C nearest neighbor distance (experimental value 1.420 Å). The Na adsorption energies obtained show that a $5\times 5\times 1$ mesh is adequate (see also Table I), whereas the forces are already well converged for the $2\times 2\times 1$ mesh. We have also tested whether it is possible to use a smaller kinetic energy cutoff: In comparison with 70 Ry, a calculation with 50 Ry yielded 0.17 eV (33 %) weaker binding of Na, and the related perpendicular distance from the surface increased by 0.19 Å (7.8 %). This shows that the computational cost cannot be reduced without losing accuracy.

The effect of substrate relaxation has been studied by releasing the six nearest C atoms and reoptimizing the Na-HOPG system geometry. The changes are small (e.g. the C-C distance 1.424 Å) which validates the use of fixed substrate in real applications. A benchmark calculation for Na-HOPG shows that the local spin density (LSD) approximation does not improve the results because of the large number of KS states involved and the nonmagnetic nature of the system. The calculations below are done with spin-degenerate KS orbitals except for isolated Na atom and Na clusters.

III. RESULTS

In order to map the potential energy surface of a Na-HOPG system, we have optimized the Na atom position for different locations along the surface (see Fig. 2). The results for adsorption energy (ΔE_{\perp}), separation from the surface (d_{\perp}), nearest carbon atom distances (Na-C), and carbon coordination numbers (N_C) are presented in Table I. Here, we do not approach the real zero-density limit of Na, but the atoms are distributed in 9.84×8.53 Å intervals due to the periodic boundary conditions applied.³⁵ Inclusion of more \mathbf{k} -points enhances binding in a systematic way yielding to an estimate of 0.51 eV for the energy minimum (point 0, $5\times 5\times 1$ mesh). Comparison with other locations shows only small deviations in ΔE_{\perp} and d_{\perp} , indicating a flat potential energy surface with a maximum variation of 0.07 eV. The points 2 and 4 above C_{α} and C_{β} (Fig. 2) give similar results, which causes increased symmetry in the PES. These findings resemble the results by Lamoen and Persson⁸ who obtained $\Delta E_{\perp} = 0.52$ eV for a K-HOPG system and a small diffusion barrier (variation 0.05 eV). No \mathbf{k} -points were used in these calculations, but we expect a systematic shift in ΔE_{\perp}

similar to the one we found.

Table II shows the formation energetics of Na atoms and clusters. The formation energy ΔE is divided into two components: the binding energy of a free cluster or a separated monolayer (ΔE_b), and a term (ΔE_\perp) describing the adsorption energy. Three phases of Na-HOPG are included in Table II, where Na(I) refers to the initial sparse system, Na(II) is a commensurate periodic structure with twice as many Na atoms per unit shell as Na(I) (Na-Na separation 6.51 Å), and Na(III) corresponds to the (2×2) Na monolayer with four times the coverage of Na(I) and hexagonal symmetry. The phase Na(II) was encountered as a byproduct of Na₂ stretching, and it corresponds to the maximal separation of Na atoms allowed by the smaller supershell used. The effect of nearby Na atoms becomes clear in Na(III), where the separation from the surface is 0.76 Å greater. The loss in surface binding is compensated by the interaction with other Na atoms, and the resulting ΔE per atom is slightly larger than for Na(I). A similar (2×2) structure is stable for potassium,⁹ and theoretical studies have shown that K forms a metallic state on HOPG.^{6,7,8} Our results corroborate this finding, but – in the case of Na monolayer – the spacing between Na atoms (4.92 Å) does not match typical Na-Na distances (see Na clusters in Table III), and the energy difference with the lower coverage phase Na(I) is relatively small.

The cluster formation energies in Table II reveal significant differences between individual clusters. Na₂ binds only very weakly due to its closed valence electron shell, and the dimer separation from the surface is 1 Å larger than for Na₃ and Na₄. The same effect is apparent in the ΔE_\perp values. It is interesting that the deviation of ΔE for 2×2×1 and 5×5×1 **k**-point meshes becomes smaller as the distance between Na atoms and surface increases (see e.g. Na₃). This implies changes in charge transfer. The larger substrate used for Na₄ and Na₅ requires fewer **k**-points to converge the formation energy, which can be seen as nearly identical ΔE values. The ΔE values of Na₃, Na₄, and Na₅ are larger than for the (2×2) Na monolayer, which shows that the clustering of Na atoms is preferred.

The optimized cluster structures are related to the ground state geometries of free Na clusters. For Na₃, Na₄, and Na₅ the corresponding isomers are an isosceles triangle, a rhombus, and a planar C_{2v} isomer. The clusters are placed on HOPG in a way that assumes that the hollow site (point 0) is energetically favorable for each Na atom. The related bond distances, angles, torsional angles, and distances from the surface are given in Table III. As mentioned above, Na₂ binds weakly, and this can also be seen in the very small change in

dimer bond length (0.02 Å). For the other clusters changes are more obvious: Na₃ adopts a geometry close to an equilateral triangle with significant changes in bond lengths and angles. Na₄ bends away from planarity (torsional angle 8.7°), and the bond lengths increase systematically, but the angles remain close to the initial values. For Na₃ all atoms occupy similar sites on top of point 5 (see Figs. 1, 2), not far from hexagon centers. The atoms of Na₄ are coordinated with HOPG in two ways: the two corners of the rhombus are above C atoms and bent towards the substrate (a result contradictory to the PES of Na(I)), whereas the other two Na atoms are close to the hexagon centers. The geometry and position of Na₄ is shown in an electron density isosurface plot in Fig. 3.

The adsorption of Na₅ leads to a significant distortion from planarity, with the central Na atom being much farther from the surface (0.69 Å) than the other atoms. Simultaneously, the longest Na-Na bond is broken (4.11 Å, see Table III), and the resulting C_s structure (Fig. 4) comprises two identical triangles connected via their apices. As for the other clusters, changes in bond lengths are considerable, and there are also changes in bond angles. The Na atoms are coordinated with the surface in three ways: the central atom is on a hollow site, the two atoms that initially comprised the broken Na-Na bond sit on top of C-C bonds, and the two corner atoms are directly above C atoms. Here, we have optimized the cluster geometry with respect to a substrate consisting of two graphene layers alone (120 C atoms).³⁶ The obvious changes are an increased separation of the middle Na atom from the surface (0.20 Å) and a further elongation of the longest (broken) Na-Na bond (0.11 Å). The other bond distances and the formation energy ΔE are unchanged.

The electron density isosurface plot of Na₅-HOPG in Fig. 4 illustrates how the density is distributed within the Na₅ cluster. The largest values are obtained inside the two remaining triangles, but there is a component also in the interstitial region next to the broken (or elongated) Na-Na bond. The Na atom in the middle has a pronounced hole in the density, but an atom-centered integration of charge density within a small spherical volume ($R = 1.5$ Å) gives similar results (charges) for each Na atom. This is explained by the fact that the most coordinated Na atom has density contributions from both triangles. Presumably, this atom prefers a larger distance from the surface and a hollow site because of its higher Na coordination, whereas the lower coordinated Na atoms tend to acquire positions closer to carbons and C-C bonds. The same applies to Na₄ but on a smaller scale (see Fig. 3).

We have listed on Table IV formation energies for different cluster/atom products on

top of the HOPG substrate, calculated assuming an initial state of N free Na atoms in the gas phase. The most obvious feature is the small formation energy of Na_2 containing products. This is caused by the full valence electron shell of Na_2 that reduces binding with the substrate. Even two separated Na atoms are more stable on graphite than a dimer. For larger systems Na_3 , Na_4 , and Na_5 are favored, indicating clustering processes, and the product Na_3+Na is slightly higher in formation energy than Na_4 . The unpaired electron on the outermost shell of Na_3 (and Na) increases binding with HOPG as seen in Table II. A similar conclusion can be made about the high stability of Na_5 . This indicates that open shell clusters can be more abundant on graphite than in the gas phase.

The weak binding of Na_2 compared to two separated atoms has suggested to us to investigate the breaking of this bond. For this purpose the Na_2 bond distance has been increased gradually up to a point where the periodic Na(II) phase is obtained. Each configuration has been optimized with respect to the surface, and the total energy is calculated with the $5\times 5\times 1$ \mathbf{k} -point mesh. Our results show a monotonic increase up to Na(II), which is the upper limit of Na-Na distance (6.51 Å) in the supershell chosen. At this point, the energy is 0.30 eV higher, which should be considered as the lower bound of the Na_2 dissociation energy on HOPG. This is still significantly less than the gas phase value 0.68 eV, but the substrate now causes the interaction between Na atoms to be long-ranged. On the other hand, Na_2 stretches readily; as the Na-Na separation is increased to 4.26 Å where both atoms sit on a hollow site (second nearest hexagons) the total energy change is only 0.09 eV, but the distance $d_{\perp}=3.09$ Å is 0.86 Å less. This suggests that Na_2 on graphite has very low frequency vibrational modes in both lateral and perpendicular directions.

Charge transfer between the adsorbate and the substrate is studied in detail in the case of Na-HOPG and Na_3 -HOPG,³⁷ and the laterally averaged charge density differences ($\Delta\rho$) are presented in Fig. 5. In both cases, the oscillating profile of $\Delta\rho$ shows that the presence of adsorbate affects the whole system including the lowermost (third) graphene layer. The negative node close to the Na/ Na_3 indicates a charge transfer to the substrate that is partially counterbalanced by the strong positive peak next to the first graphene layer (GR1, see Table V). The location and shape of the negative node is different for Na and Na_3 : for a single atom the charge is depleted throughout the whole atomic volume causing a broad minimum in $\Delta\rho$, whereas for Na_3 the minimum is deeper and biased to the lower side of the cluster. Integration over this area gives values $\Delta q = -0.47$ e and $\Delta q = -0.48$ e for Na and Na_3 ,

respectively. The similar Δq values indicate that the substrate does not support more excess charge, and it explains the increased d_{\perp} for Na₃, Na₄, Na₅ and (2×2) Na monolayer.

A layer-by-layer analysis of the graphite substrate in Table V shows that the charge transferred is distributed over the three layers. In comparison with the middle layer (GR2), Δq is slightly larger for the lowermost layer (GR3). This is probably a finite-size effect, a conclusion that is supported by the $\Delta\rho$ profile. The inclusion of \mathbf{k} -points leads to more pronounced oscillations near GR2 and GR3, whereas GR1 has more accumulated charge in the Γ -point approximation. This shows that the charge transferred becomes more delocalized as \mathbf{k} -points are introduced in the lateral dimension. The Γ -point approximation underestimates the amount of charge transfer also for Na, whereas for Na₃ the values are similar. Lamoen and Persson⁸ found $\Delta q = -0.40$ e for a (4×4) K monolayer, which agrees with our result $\Delta q = -0.39$ for a corresponding density of Na using a single Γ -point (Table V).

The electronic densities of valence states (DOS) of Na₅-HOPG and HOPG are plotted in Fig. 6. The calculations were done using a 5×5×1 Monkhorst-Pack \mathbf{k} -point mesh, and the KS eigenvalues obtained are interpolated to correspond a 9×9×1 mesh (this resembles the common tetrahedron method)³⁸. The DOS of graphite substrate shows typical features,^{1,2} including a steep rise at -20 eV due to the 2D character of graphite, a dip at -13 eV after the first two σ bands, a large peak at -6.5 eV followed by a shoulder in the decreasing profile with zero weight and zero gap at the Fermi energy. Our substrate model then captures the relevant properties of graphite, although the system is finite in the perpendicular direction.

A very small effect is observed due to the Na₅ adsorption, and the characteristic features of graphite substrate are clearly visible. The conduction band is now being filled by the Na₅ valence electrons, which can be seen as a small peak at the Fermi energy. The band structure of the three (spin-degenerate) Na₅-HOPG conduction states reveals that the dispersion of the first does not correspond to its graphite counterparts (π^* bands), but resembles more the valence states (π bands). This is not true for the two other conduction states, where the lower one shows only minor variation as a function of \mathbf{k} , and the higher one resembles closely the graphite conduction bands. The two uppermost valence states are also affected by the presence of Na₅, which can be seen as smaller dispersion. Together with the lowest conduction state, this results in a small hump in the DOS next to the minimum separating conduction and valence bands.

IV. CONCLUSION

We have studied Na atoms and small Na clusters ($N \leq 5$) on graphite using a DFT method that uses pseudopotentials and periodic boundary conditions. In order to obtain reliable results the simulated slab of graphite consists of three graphene layers, and is sufficiently large to yield an appropriate separation between the adsorbate replica in lateral dimension. In addition, a high kinetic energy cutoff (70 Ry) for the plane wave basis set and \mathbf{k} -points make the calculations very demanding in terms of CPU time and memory.

For a dispersed phase, an Na atom has an adsorption energy of 0.51 eV at the hollow site 2.45 Å above the surface. The small diffusion barrier of 0.06 eV shows that the potential energy surface of the Na atom is flat. These results are similar to the recent results for NaC₆₀ compounds, where an adsorption energy of 0.65 eV and a diffusion barrier of 0.07 eV were observed at the hexagonal site.³⁹ A higher Na coverage leads to a decreased interaction with the substrate as shown for the (2×2) monolayer ($d_{\perp} = 3.21$ Å). The dispersed phase and (2×2) monolayer differ little energetically, and neither is found to be stable experimentally. Instead, the calculated cluster formation energies favor clustering processes (island formation) in agreement with experiment.^{6,12,13} The formation energies of the open shell systems Na, Na₃, and Na₅ are larger than those of closed shell cases Na₂ and Na₄. This is related to the spin-degeneracy of the highest molecular orbital (odd-even staggering) and, in contrast to free metal clusters, gives rise to increased stability of odd cluster sizes on HOPG.

A charge density analysis for Na and Na₃ shows that approximately 0.5 electrons are transferred to the substrate in both cases, indicating that HOPG does not support much excess charge, and that polarization effects weaken as the Na coverage is increased. As shown before for K,^{6,7,8} this leads to decoupling between the adsorbate and substrate, and a two-dimensional metallic film on HOPG results. In the case of Na clusters, the partial loss in electron density is evident in significant changes in cluster geometries. For example, Na₃ is more like a closed shell Na₃⁺ ion, and consequently, the geometry is closer to an equilateral triangle than that of a free Na₃. An interesting observation is that the planarity of Na₄ and Na₅ is broken as the atoms having more Na-Na bonds move farther from the surface. Whether this is related to the experimentally observed buckling of Na overlayers remains an open question.^{9,12}

V. ACKNOWLEDGMENTS

This work has been supported by the Academy of Finland under the Finnish Centre of Excellence Programme 2000-2005 (Project No. 44875, Nuclear and Condensed Matter Programme at JYFL). The calculations were performed on the IBM-SP4 computers at the Center for Scientific Computing, Espoo, Finland. J.A. has been supported by the Bundesministerium für Bildung und Forschung (BMBF), Bonn, within the Kompetenzzentrum Materialsimulation, 03N6015. We thank R.O. Jones for valuable discussions and critical reading of the manuscript.

-
- ¹ J.-C. Charlier, X. Gonze, and J.-P. Michenaud, *Phys. Rev. B* **43**, 4579 (1991).
 - ² J.-C. Charlier, J.-P. Michenaud, and X. Gonze, *Phys. Rev. B* **46**, 4531 (1992).
 - ³ J.C. Boettger, *Phys. Rev. B* **55**, 11202 (1997).
 - ⁴ K.R. Kganyago and P.E. Ngoepe, *Phys. Rev. B* **68**, 205111 (2003).
 - ⁵ M.R.C. Hunt and R.E. Palmer, *Phil. Trans. R. Soc. Lond. A* **356**, 231 (1998).
 - ⁶ J.D. White, J. Cui, M. Strauss, R.D. Diehl, F. Ancilotto, and F. Toigo, *Surf. Sci.* **307-309**, 1134 (1994).
 - ⁷ F. Ancilotto and F. Toigo, *Phys. Rev. B* **47**, 13713 (1993).
 - ⁸ D. Lamoen and B.N.J. Persson, *J. Chem. Phys.* **108**, 3332 (1998).
 - ⁹ M. Breitholtz, T. Kihlgren, S.-Å. Lindgren, and L. Waldén, *Phys. Rev. B* **66**, 153401 (2002).
 - ¹⁰ E. Cheng, M. W. Cole, W. F. Saam, and J. Treiner, *Phys. Rev. Lett.* **67**, 1007 (1991).
 - ¹¹ Z. P. Hu and A. Ignatiev, *Phys. Rev. B* **30**, 4856 (1984).
 - ¹² M. Breitholtz, T. Kihlgren, S.-Å. Lindgren, H. Olin, E. Wahlström, and L. Waldén, *Phys. Rev. B* **64**, 073301 (2001).
 - ¹³ M. Breitholtz, T. Kihlgren, S.-Å. Lindgren, and L. Waldén, *Phys. Rev. B* **67**, 235416 (2003).
 - ¹⁴ Z. P. Hu, N. J. Wum and A. Ignatiev, *Phys. Rev. B* **33**, 7683 (1986).
 - ¹⁵ M.R.C. Hunt, P.J. Durston, and R.E. Palmer, *Surf. Sci.* **364**, 266 (1996).
 - ¹⁶ N. J. Wu and A. Ignatiev, *J. Vac. Sci. Technol.* **20**, 896 (1982).
 - ¹⁷ Z. Y. Li, K. M. Hock, and R. E. Palmer, *Phys. Rev. Lett.* **67**, 1562 (1991).
 - ¹⁸ R.E. Palmer, S. Pratontep, and H.-G. Boyen, *Nature materials* **2**, 443 (2003).

- ¹⁹ L. Lou, L. Österlund, and B. Hellsing, *J. Chem. Phys.* **112**, 4788 (2000).
- ²⁰ D.M. Duffy and J.A. Blackman, *Surf. Science* **415**, L1016 (1998).
- ²¹ D.M. Duffy and J.A. Blackman, *Phys. Rev. B* **58**, 7443 (1998).
- ²² J.-F. Gal, P.-C. Maria, M. Decouzon, O. M6, M. Y6a6nes, and J.L.M. Abboud, *J. Am. Chem. Soc.* **125**, 10394 (2003).
- ²³ O. Hjortstam, J.M. Wills, B. Johansson, and O. Eriksson, *Phys. Rev. B* **58**, 13191 (1998).
- ²⁴ I. Moullet, *Surf. Sci.* **331-333**, 697 (1995).
- ²⁵ F. Hagelberg, P. Scheier, B. Marsen, M. Lonfat, and K. Sattler, *J. Mol. Struc. (Theochem)* **529**, 149 (2000).
- ²⁶ F. Hagelberg, C. Xiao, B. Marsen, M. Lonfat, P. Scheier, and K. Sattler, *Eur. Phys. J. D* **16**, 37 (2001).
- ²⁷ D.C. Sorescu, K.D. Jordan, and P. Avouris, *J. Phys. Chem.* **105**, 11227 (2001).
- ²⁸ P. Giannozzi, R. Car, and G. Scoles, *J. Chem. Phys.* **118**, 1003 (2003).
- ²⁹ Y. Ferro, F. Marinelli, and A. Allouche, *J. Chem. Phys.* **116**, 8124 (2002).
- ³⁰ CPMD V3.5 Copyright IBM Corp 1990-2002, Copyright MPI f6r Festk6rperforschung Stuttgart 1997-2001.
- ³¹ N. Troullier and J.L. Martins, *Phys. Rev. B* **43**, 1993 (1991).
- ³² J.P. Perdew, K. Burke, and M. Ernzerhof, *Phys. Rev. Lett.* **77**, 3865 (1996).
- ³³ H.J. Monkhorst and J.D. Pack, *Phys. Rev. B* **13**, 5188 (1976).
- ³⁴ Especially the distance from the surface is sensitive to the number of graphene layers. For two graphene layers the distance is 0.16 Å (6.6 %) larger than for three and four layers.
- ³⁵ This system corresponds to a (4×4) Na monolayer in terms of coverage.
- ³⁶ The corresponding box size 12.30×12.79×13.35 Å³.
- ³⁷ The value of charge transfer can depend on the method used for its determination. We use the same method as the previous studies on alkali-HOPG systems.^{6,7,8}
- ³⁸ Ph. Lambin and J.P. Vigneron, *Phys. Rev. B* **29**, 3430 (1984).
- ³⁹ J. Roques, F. Calvo, F. Spiegelman, and C. Mijoule, *Phys. Rev. B* **68**, 205412 (2003).

Figures

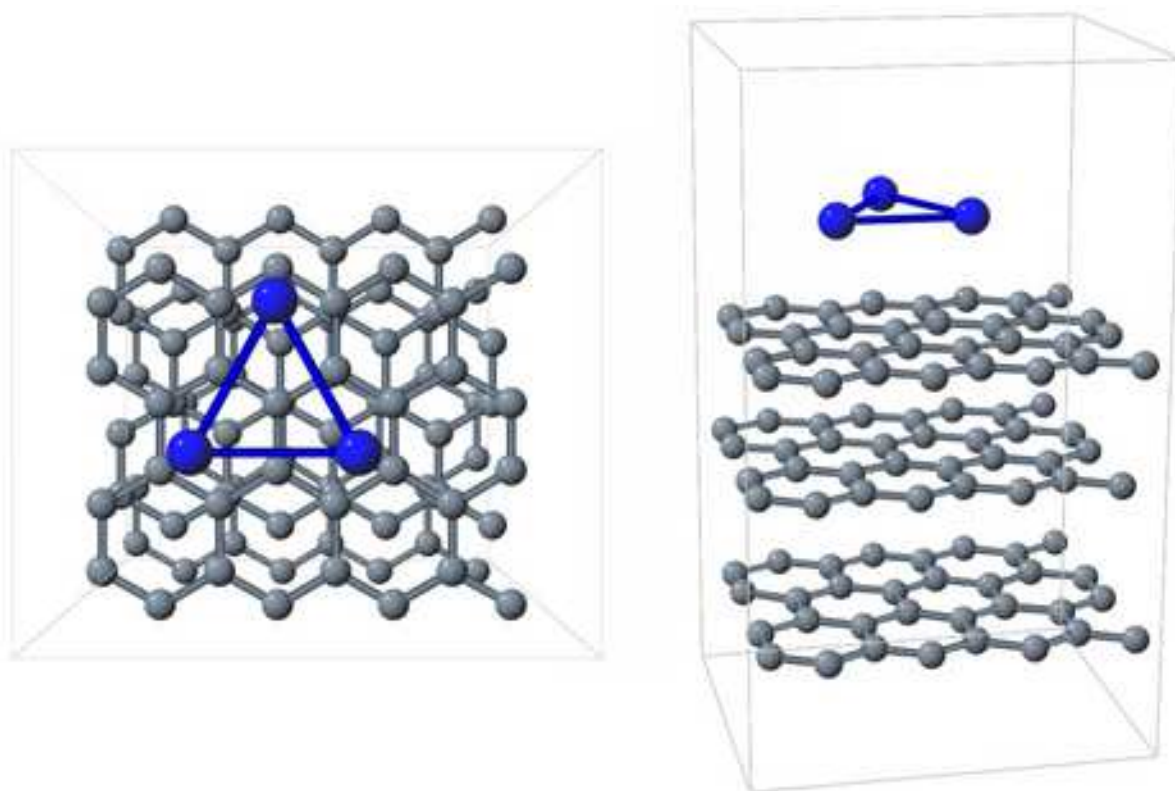


FIG. 1: Optimized Na₃-HOPG system shown from two perspectives. The supershell size is $9.84 \times 8.53 \times 16.70 \text{ \AA}^3$. Each graphene layer consists of 32 atoms.

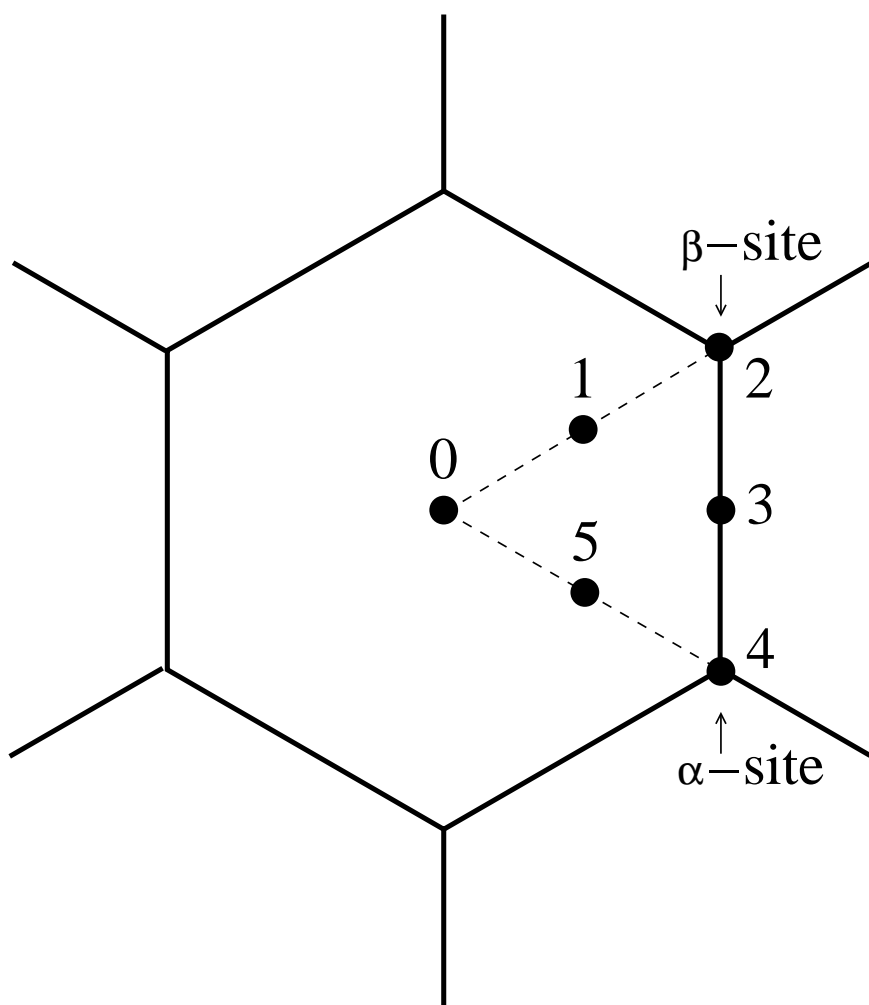


FIG. 2: Numbered locations of Na atom on top of a graphite hexagon.

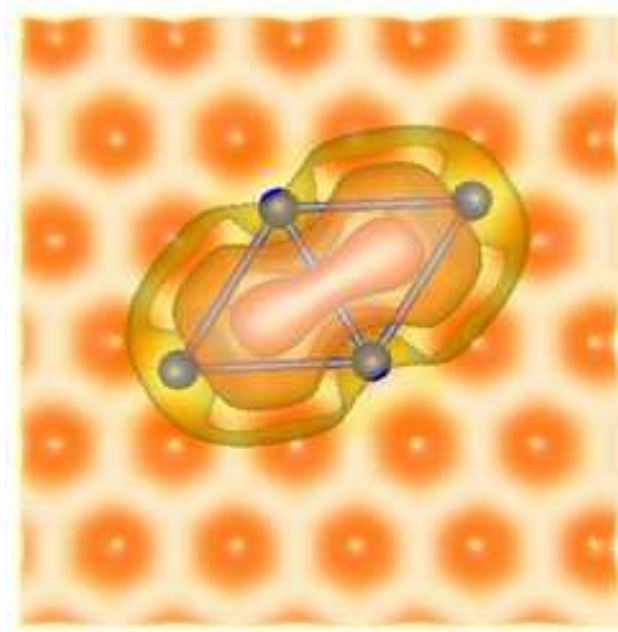


FIG. 3: Three density isosurfaces for Na_4 -HOPG system. The corresponding density values are 0.002 (yellow), 0.004 (orange), and 0.007 au (red), respectively. The accumulated charges within the cluster are 1.77, 0.98, and 0.14 e, respectively.

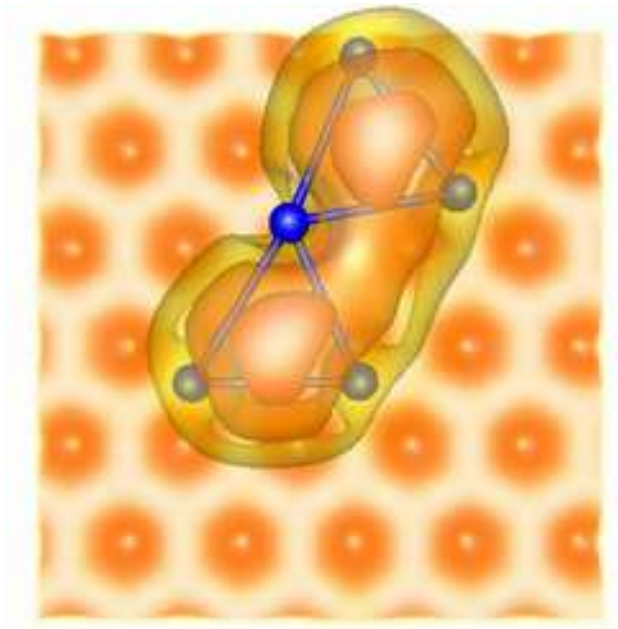


FIG. 4: Three density isosurfaces for Na_5 -HOPG system. The corresponding density values are 0.002 (yellow), 0.004 (orange), and 0.007 au (red), respectively. The accumulated charges within the cluster are 2.37, 1.44, and 0.35 e, respectively.

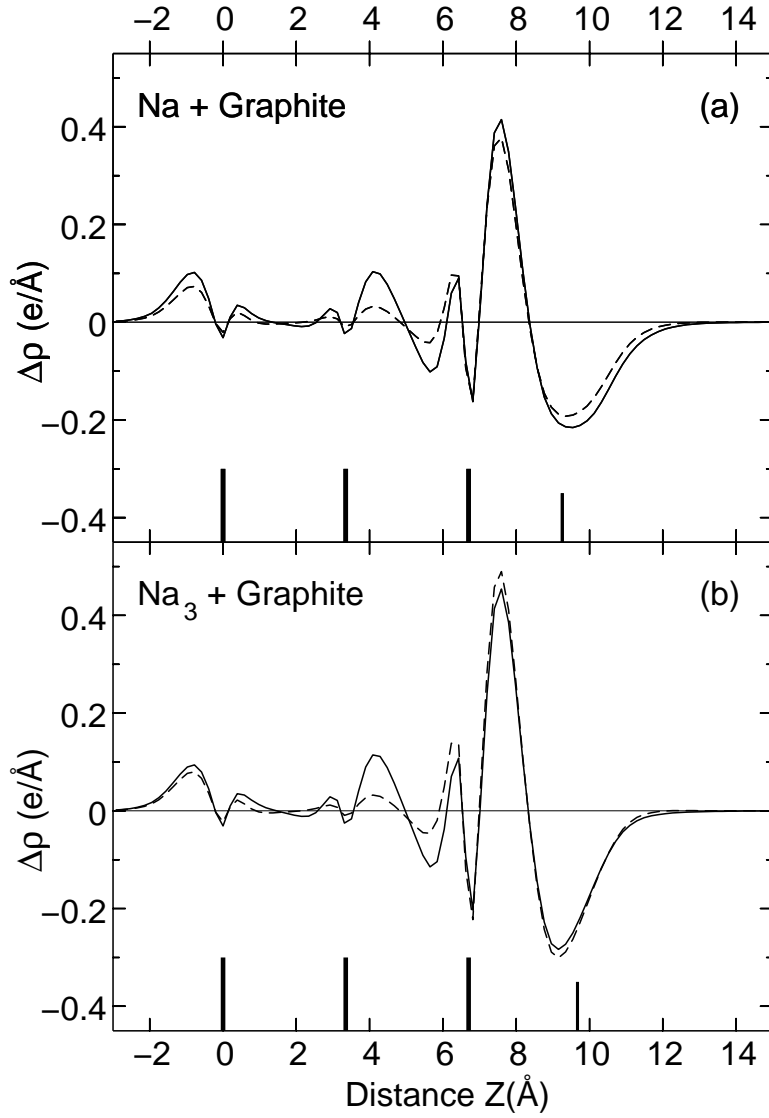


FIG. 5: Laterally averaged charge density difference for (a) Na-HOPG and (b) Na₃-HOPG systems. The solid and dashed lines mark the $5 \times 5 \times 1$ \mathbf{k} -point mesh and the Γ -point approximation, respectively. The thick vertical bars denote the positions of graphene layers (longer bars) and Na/Na₃ (shorter bar).

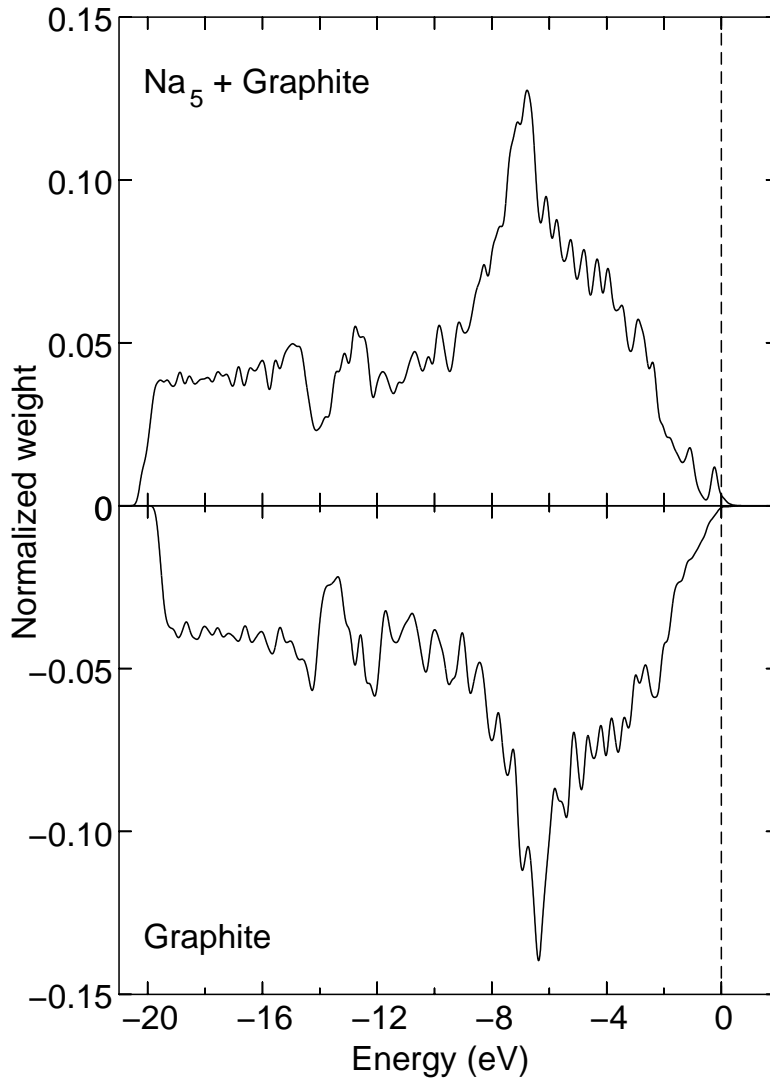


FIG. 6: Normalized DOS of Na₅-HOPG and HOPG systems calculated with the $5 \times 5 \times 1$ \mathbf{k} -point mesh. The data is interpolated to correspond a $9 \times 9 \times 1$ mesh, and Gaussians of 0.10 eV width were used for each data point. The dashed line marks the Fermi level.

Tables

TABLE I: Na atom on graphite (0001) at different locations. ΔE_{\perp} is calculated for both the $2\times 2\times 1$ and $5\times 5\times 1$ \mathbf{k} -point meshes, but the geometries are optimized using the $2\times 2\times 1$ mesh alone. The vertical distance from the graphite layer (d_{\perp}), the Na-C distance, and the carbon coordination number (N_C) are given also.

Point	ΔE_{\perp} (eV)	d_{\perp} (Å)	Na-C (Å)	N_C
0	0.12/0.51	2.45	2.83	6
1	0.08/0.47	2.49	2.59, 2.78	3
2	0.06/0.44	2.53	2.53	1
3	0.07/0.45	2.53	2.63	2
4	0.06/0.44	2.54	2.54	1
5	0.09/0.47	2.50	2.60, 2.78	3

TABLE II: Na atoms and clusters on graphite (0001). ΔE and ΔE_{\perp} are calculated for both the $2\times 2\times 1$ and $5\times 5\times 1$ \mathbf{k} -point meshes, but the geometries are optimized using the $2\times 2\times 1$ mesh alone.

	$\Delta E/\text{atom}$ (eV)	$\Delta E_b/\text{atom}$	$\Delta E_{\perp}/\text{atom}$	d_{\perp} (Å)
Na(I)	0.12/0.51	—	0.12/0.51	2.45
Na(II)	0.15/0.33	0.09	0.07/0.24	2.81
Na(III)	0.46/0.57	0.19	0.27/0.38	3.21
Na ₂	0.40/0.48	0.34	0.06/0.14	3.95
Na ₃	0.56/0.68	0.35	0.21/0.34	2.95, 2.98
Na ₄ [†]	0.65/0.64	0.45	0.20/0.19	2.88, 3.12
Na ₅ [†]	0.68/0.71	0.46	0.22/0.25	3.08, 3.77

[†]larger substrate of 60 atoms per layer and simulation box of $12.30\times 12.79\times 16.70$ Å³

TABLE III: Optimized structures of adsorbed Na clusters. Distances in Ångström and angles in degrees. The values in parentheses refer to the gas phase structures.

	Na ₂	Na ₃	Na ₄	Na ₅
Na-Na	3.07 (3.05)	3.35 (3.17)	3.53 (3.43)	3.24 (3.33)

	3.26 (3.97)	3.27 (3.02)	3.34 (3.42)	
			3.62 (3.36)	
			4.11 (3.46)	
d_{\perp}	3.95	2.95, 2.98	2.88, 3.12	3.08, 3.77
Na-C	4.52	3.10	2.92, 3.30	3.09-4.12
Angle		58.2 (77.7)	55.2 (52.2)	58.1 (61.8)
			62.4 (63.7)	66.7 (59.5)
			124.2 (127.8)	55.3 (58.7)
				75.9 (60.5)
				155.2 (177.7)
Torsion			8.7	14.9, 30.7

TABLE IV: Formation energies of Na products on graphite (0001). A large separation of end products is assumed.

Reactants (free)	Products (graphite)	ΔE (eV)
Na	Na	0.51 eV
2×Na	Na ₂	0.96 eV
	2×Na	1.02 eV
3×Na	Na ₃	2.05 eV
	Na ₂ + Na	1.47 eV
	3×Na	1.53 eV
4×Na	Na ₄	2.55 eV
	Na ₃ + Na	2.56 eV
	Na ₂ + Na ₂	1.92 eV
	Na ₂ + 2×Na	1.98 eV
	4×Na	2.04 eV
5×Na	Na ₅	3.54 eV
	Na ₄ + Na	3.06 eV
	Na ₃ + Na ₂	3.01 eV

$\text{Na}_3 + 2 \times \text{Na}$	3.07 eV
$5 \times \text{Na}$	2.55 eV

TABLE V: Charge transfer in Na-HOPG and Na_3 -HOPG (in electrons). The values in parenthesis are for the Γ -point approximation.

	Na	GR1	GR2	GR3
Na-HOPG	-0.47 (-0.39)	0.25 (0.28)	0.09 (0.03)	0.13 (0.09)
Na_3 -HOPG	-0.48 (-0.49)	0.26 (0.37)	0.10 (0.03)	0.12 (0.09)